

Forensic engineering methodology to assess the Maintenance, Repair and Overhaul (MRO) procedures for Gas Generator Turbine Cooling Plates

D.G.Karalis^a and N.E.Melanitis^a

^aHellenic Navy, Hellenic Naval Academy, Mechanics & Materials Division, Marine Materials Laboratory, Hazjikyriakou Avenue, Piraeus 185 39, Greece

Abstract. Investigation was carried out on a set of cooling plates obtained from a gas generator turbine (GGT). The need for the assessment of the durability and remaining operational life of the gas generator turbine component was identified, following a recommendation by the manufacturer for the early replacement of the cooling plates. The current study applied a forensic engineering and failure analysis methodology to assess the Maintenance, Repair and Overhaul (MRO) procedures of high reliability components. From the results of the current investigation it was finally deduced that, in spite the fact that the plates seemed to be macroscopically in good condition, certain metallurgical observations sustained the claim for early component replacement.

Keywords: Gas generator turbine, cooling plate, coated nickel superalloy, failure analysis, forensic engineering methodology.

INTRODUCTION

A set of eight cooling plates from a gas generator turbine were delivered to the Marine Materials Laboratory following a recommendation by the manufacturer for earlier replacement due to changes to the specifications. The eight cooling plates were obtained from an engine that is depicted schematically in figure 1.

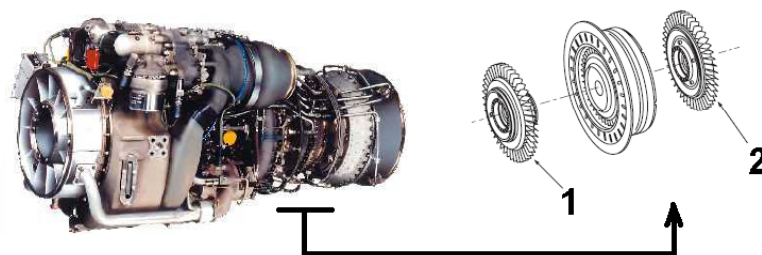


FIGURE 1. General view of the engine (left) and part of the gas generator turbine (right).

The engine consists of the compressor (cold section), the gas generator turbine (hot section) and the power turbine (power turbine section). The gas generator turbine contains the stage 1 gas generator turbine rotor (item 1 in figure 1), the stage 2 gas generator turbine rotor (item 2 in figure 1) and the gas generator stator (shown between the items 1 and 2 in figure 1). The gas

generator turbine rotors are bolted to the compression section of the engine and as the exhaust gases turn the gas generator turbine rotor, the compressor also turns. This makes the system self-sustaining. The gas turbine and the compressor rotate at 44700 RPM whereas the power turbine rotates at 20900 RPM. The items 1 and 2 that are presented in figure 1 consist of the cooling plates, the disk and the blades. These are depicted in large scale in figure 2.

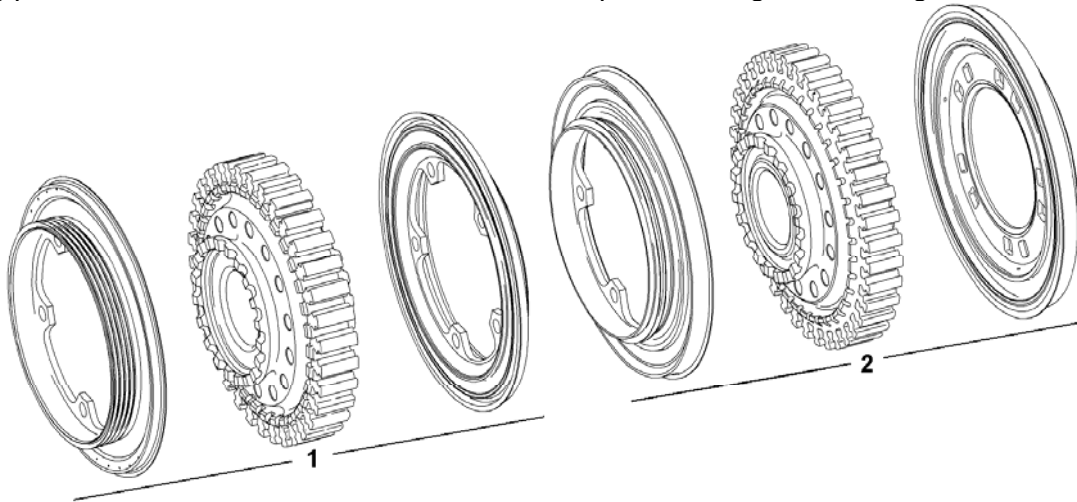


FIGURE 2. Gas generator turbine rotor parts. From left to right: stage 1 forward cooling plate, stage 1 disk (blades not shown), stage 1 aft cooling plate, stage 2 forward cooling plate, stage 2 disk (blades not shown), stage 2 aft cooling plate.

As seen from figure 2, these thin machined cooling plates are mounted on both sides of each disc in order to constrain cooling air to follow the most effective path. The plates consist of a short cylindrical body of 20 mm height and a circular flange of 148 mm diameter. The stage 1 forward cooling plate contains continuous circumferential projections along the short cylindrical body similar to a thread. The full stage 1 gas generator turbine is depicted in figure 3 (item 1 in figure 1).



FIGURE 3. The gas generator turbine rotor with the blades positioned around the rotor disk. The cooling plates are fixed with five bolts on the rotor disk. Notice the sand-color of the blades.

The aim of the current paper is to investigate whether the manufacturer recommendation for early replacement of the cooling plates was an apt advice. This will be carried out by investigating the potential existence of wear, cracking or any other evidence of structural degradation of the plates. Thus the validity of the manufacturer recommendation will be assessed and the owner of the gas generator will be consulted accordingly. In addition to the above the current study seeks to establish a set of failure analysis tools and criteria as an assessment methodology for the usability of non-failed critical engine components.

EXPERIMENTAL PROCEDURE

Macroscopic investigation was realized optically, by naked eye and by using a SSM stereomicroscope. **Microstructural analysis** was realized in mounted cross-sections of the material obtained from the flange of the disk. Manual grinding was performed using MetaServ grinding devices and successive abrasive papers up to #2400 grid followed by fine polishing using diamond and silica suspensions. Cleaning was performed using ethanol followed by hot air stream drying. Etching was performed using 7.5 mL HF, 2.5 mL HNO₃, 200 mL CH₃OH etchant. Etching time was 5 minutes. **Metallographic observation** was carried out using an AusJena metallurgical microscope. **Hardness testing** was performed employing a calibrated Indentec Rockwell A Hardness tester applying 60 kg of force. **Fractographic observation** was conducted to cleaned specimens employing a JEOL Scanning Electron Microscope. Locations for optical and electronic observation were also assisted by **Finite Element Analysis** results. Energy Dispersive X-ray Spectroscopy was used for **local chemical analysis** whereas X-ray Fluorescence was employed for **global chemical analysis** of the coating using Seiko SII, SEA 1200 VX analyzers. **Non-destructive fluorescent penetrant inspection** (Type I, Method B, Level 4) was also carried out on the cooling plates.

INVESTIGATION

Data Relevant to Cooling Plates History

The engine manufacturer recommendation for early replacement of the cooling plates was provided on the basis of advanced life-estimation numerical models results that have been recently developed by the manufacturer, as a part of its Maintenance, Repair and Overhaul (MRO) procedures. It is well understood that any premature replacement strongly influences the overall cost of the engine maintenance, whereas disregarding of the recommendation may influence the reliability of the rotor parts, the safety of the engine and crew.

Macroscopic observation

All delivered plates were in visually good condition, a fact that made the manufacturer recommendation to look excessive. Macroscopic observation carried out by naked eye on the delivered eight cooling plates did not reveal any signs of global plastic deformation or permanent global distortion. The three most strained plates (with respect to total hours in operation) had some sand deposited on their surface which is attributed to the coastal environment where the specific gas generator was operating (see the color of the whole set in

figure 3). After cleaning of the specimens it was revealed that they were deposited with a protective coating. As depicted in figure 4, in four out of the eight plates, the protective coating was worn (lost) or fractured exposing the substrate of the plate to the surrounding combustion gasses.

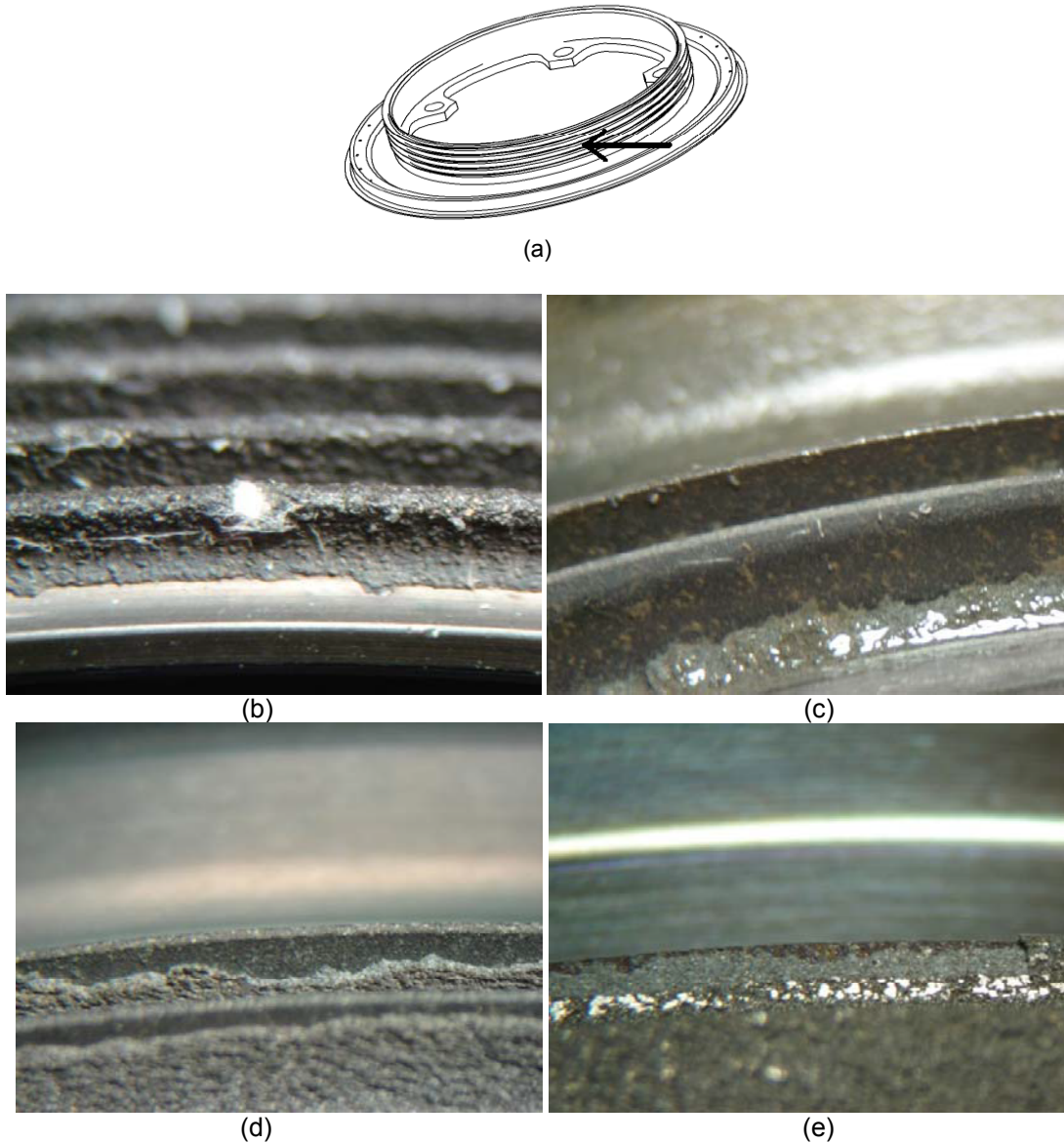


FIGURE 4. (a) Observation of the thread. (b)-(d) Existence of worn coating (lost) in three different plates. (e) In one plate the coating has been fractured.

Fracture and local plastic deformation of a structural element contained in one cooling plate was also identified as depicted in figure 5. Further detailed observation of the surface of the eight plates did not reveal any cracked areas. The latter was also confirmed by the non-destructive fluorescent penetrant inspection.

SEM Microfractography, SEM/EDS and XRF analysis

In order to further examine the plates for potential cracks and wear, Scanning Electron Microscopy was used. For this reason specimens from the most strained plate (stage 1 forward cooling plate) were prepared. Chemical analysis of a cross section of the flange (coating excluded) using SEM/EDS presented the chemical composition shown in table 1 and figure 6b.

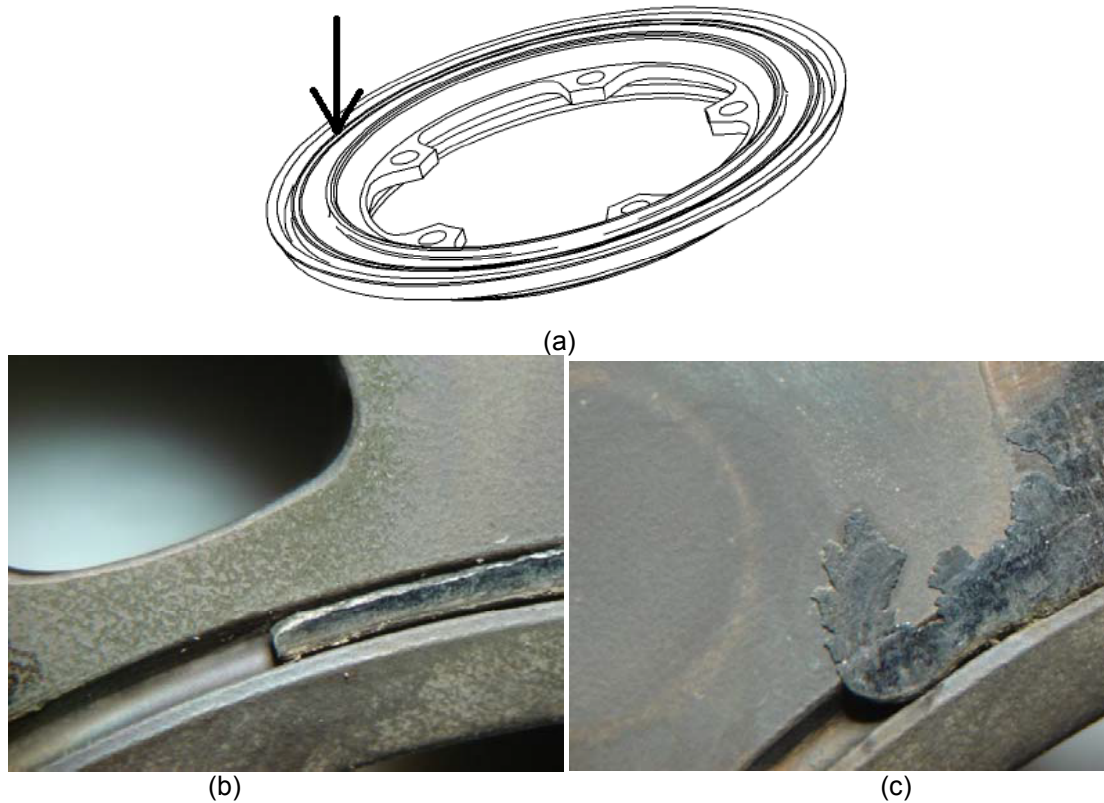


FIGURE 5. (a) Observation of the flange of one plate. (b) Fractured structural element. (c) Plastically deformed structural element.

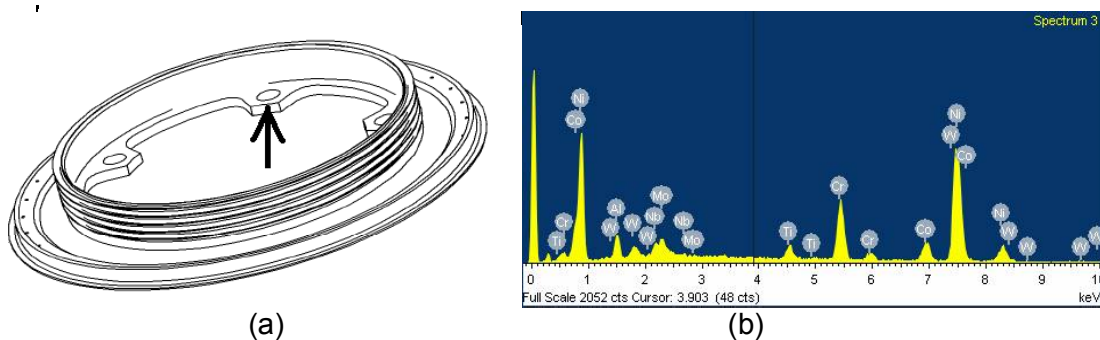


FIGURE 6. (a) Specimen location for the SEM/EDS chemical analysis. (b) Results of SEM/EDS chemical analysis

TABLE 1. Chemical composition of a cross section of the flange (coating excluded)

Element	Al	Ti	Cr	Co	Ni	Nb	Mo	W
---------	----	----	----	----	----	----	----	---

%w/w	4	3	13.5	7.5	bal	5.9	4	4
------	---	---	------	-----	-----	-----	---	---

Detailed examination of the specimens revealed the existence of worn surfaces on the plate's coating. More specifically, three different zones of non-uniform wear of the coating were identified on the flange of the plate as shown in figure 7.

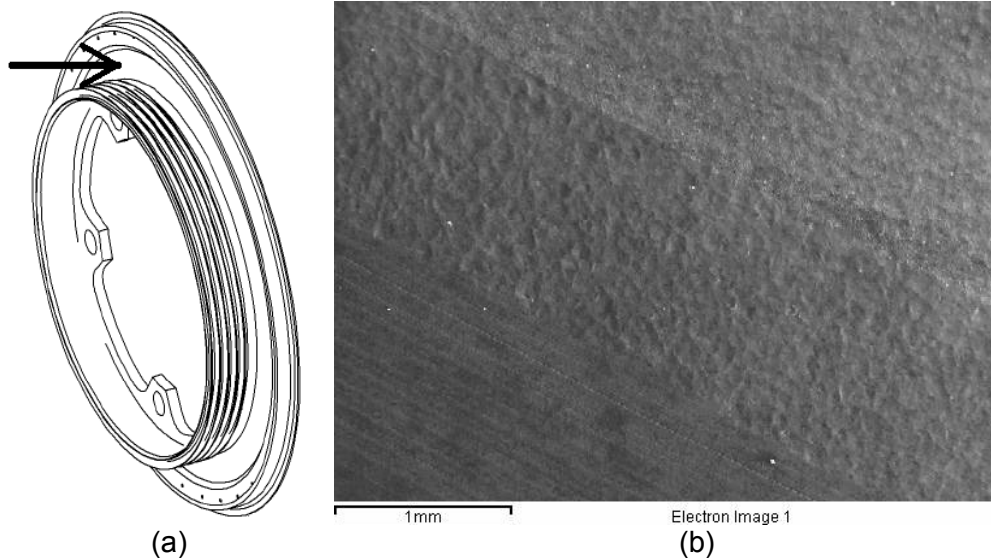


FIGURE 7. (a) Observation of the flange. (b) Existence of three different zones of non-uniform wear of the coating.

Qualitative local chemical analysis of the worn coated surface using both SEM/EDS and XRF revealed the existence of the elements shown in Table 1 plus some small amounts of Fe as shown in figure 8.

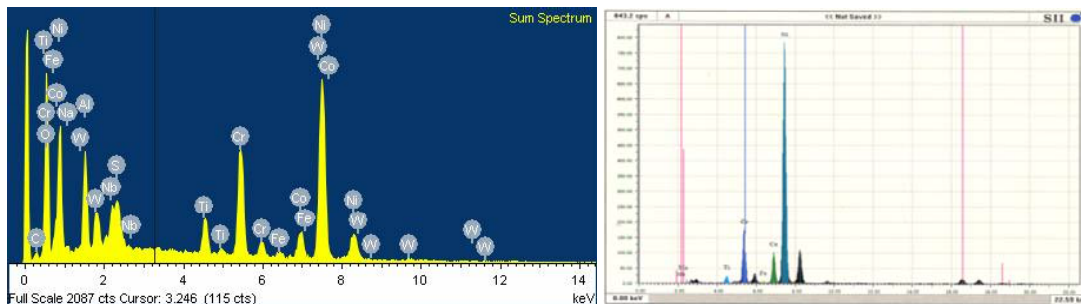


FIGURE 8. Local qualitative chemical analysis of worn coating (a) SEM/EDS results. (b) XRF results

Non uniform wear and extensive cracking was identified on the thread of the plate. More specifically, at the bottom of the thread, which is less exposed to the gasses, good coherence between the coating's matrix and the reinforcing grains was identified. Furthermore no signs of wear or cracking were existent on the coated surface. On the other hand, at the tip of the thread that is more exposed to the surrounding environment, extensive cracking, erosive wear and grain removal from the coating's matrix were identified. The results are depicted in figure 9.

The SEM/EDS chemical analysis results of the coating at the worn tip of the thread are presented in Table 2 and figure 10. No cracking was identified at any other location of the plate.

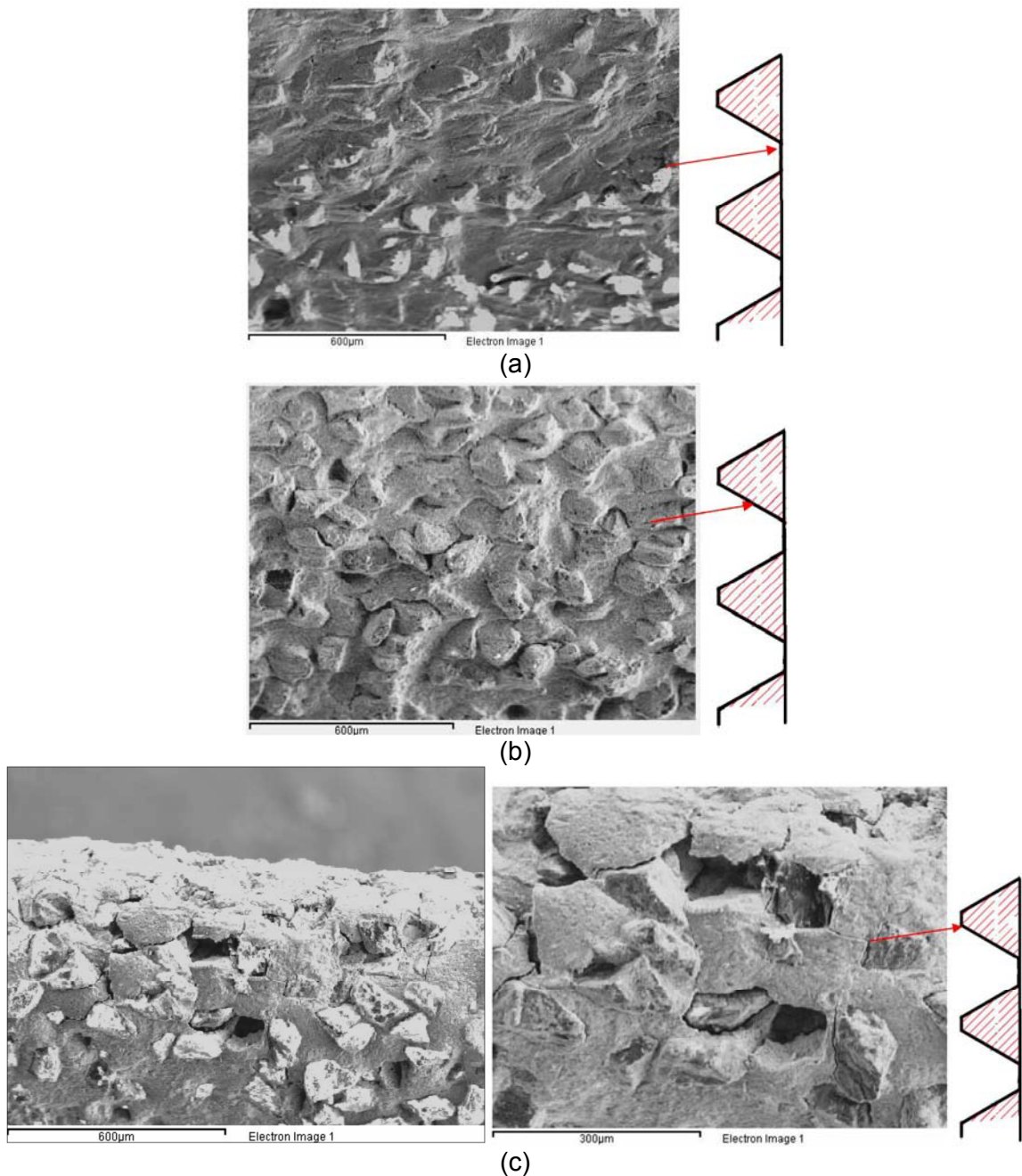


FIGURE 9. (a) Almost intact coating at the bottom of the thread. (b) The intermediate area of the thread presenting erosive wear, partial cracking and partial grain removal. (c) Tip of the thread presenting extensive cracking, erosive wear and grain removal from the coating's matrix.

TABLE 2. Chemical composition of the worn coating at the tip of the thread

Element	Al	W	Si	Fe	Ni
%w/w	11	7	23	2	bal

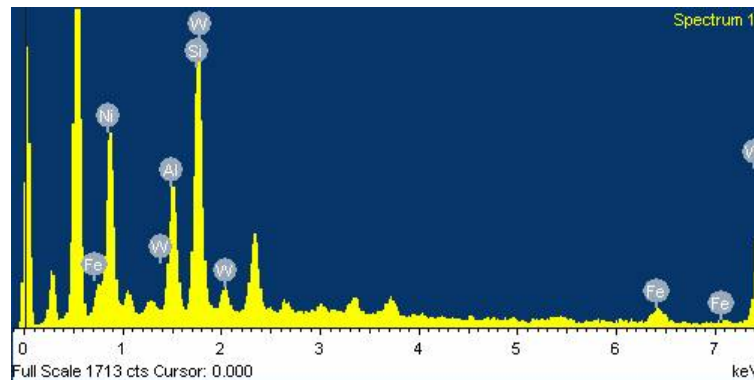


FIGURE 10. Local chemical analysis results by SEM/EDS of the worn coating at the tip of the thread

Microstructural Analysis

Specimens for microstructural analysis were prepared from a cross section of the thread of the plate in order to investigate whether the identified cracks of the coating (depicted in figure 9) have penetrated the substrate material. The investigation did not identify any cracks propagating through the substrate nickel superalloy. Strongly eroded coating and removal of the reinforcing grains from the coating's matrix were identified. The maximum thickness of the coating was measured equal to 110 μm whereas the minimum thickness was 20 μm at some locations. The analysis also revealed that the microstructure of the nickel matrix contained resolved precipitates. No blocky carbides were identified. The hardness of the plate was measured equal to 73 HRA (450 HV). The microstructural analysis results are depicted in figure 11.

Calculations and Finite Element Analysis

In order to identify the critical locations with respect to maximum stress a three dimensional linear thermo-mechanical finite element model of the most strained plate (stage 1 forward cooling plate) was set up using ALGOR® commercial code. The model contained in total 3163 flat shells (plates) and beam elements that were used to model the thread. The model was assigned with the mechanical properties of a typical Ni annealed alloy (density 8.22 gr/cm^3 , modulus of elasticity 207 GPa, Poisson ratio 0.31, thermal coefficient of expansion $13.1 \times 10^{-6} \text{K}^{-1}$ and shear modulus of elasticity 76 GPa). Coating, gas pressure, friction, rabbit loads, bolt clamp loads and manufacturing process were not included in the analysis. The nodes of the model at the holes of the flange where fixation with the disk takes place were totally fixed. The stress free reference temperature of the model was set equal to 298 K (25 °C). Two different load cases were analyzed. In load case 1 (LC1), the centrifugal loads due to rotation at nominal speed of 44700 RPM were taken into account whereas thermal strains were totally ignored. In load case 2 (LC2), the uniform temperature of the plate was set equal +100 K above the stress free reference temperature in order to let the thermal strains develop on the model, whereas the centrifugal loads were not accounted for in the analysis. The results of the FE analysis are shown in figure 12. The common 10-color contour legend refers to maximum and minimum displacement or stress: the maximum displacement of the legend refers to 0.2 mm whereas the minimum to 0 mm. The maximum stress of the legend refers to 1158 MPa whereas the minimum to -1158 MPa.

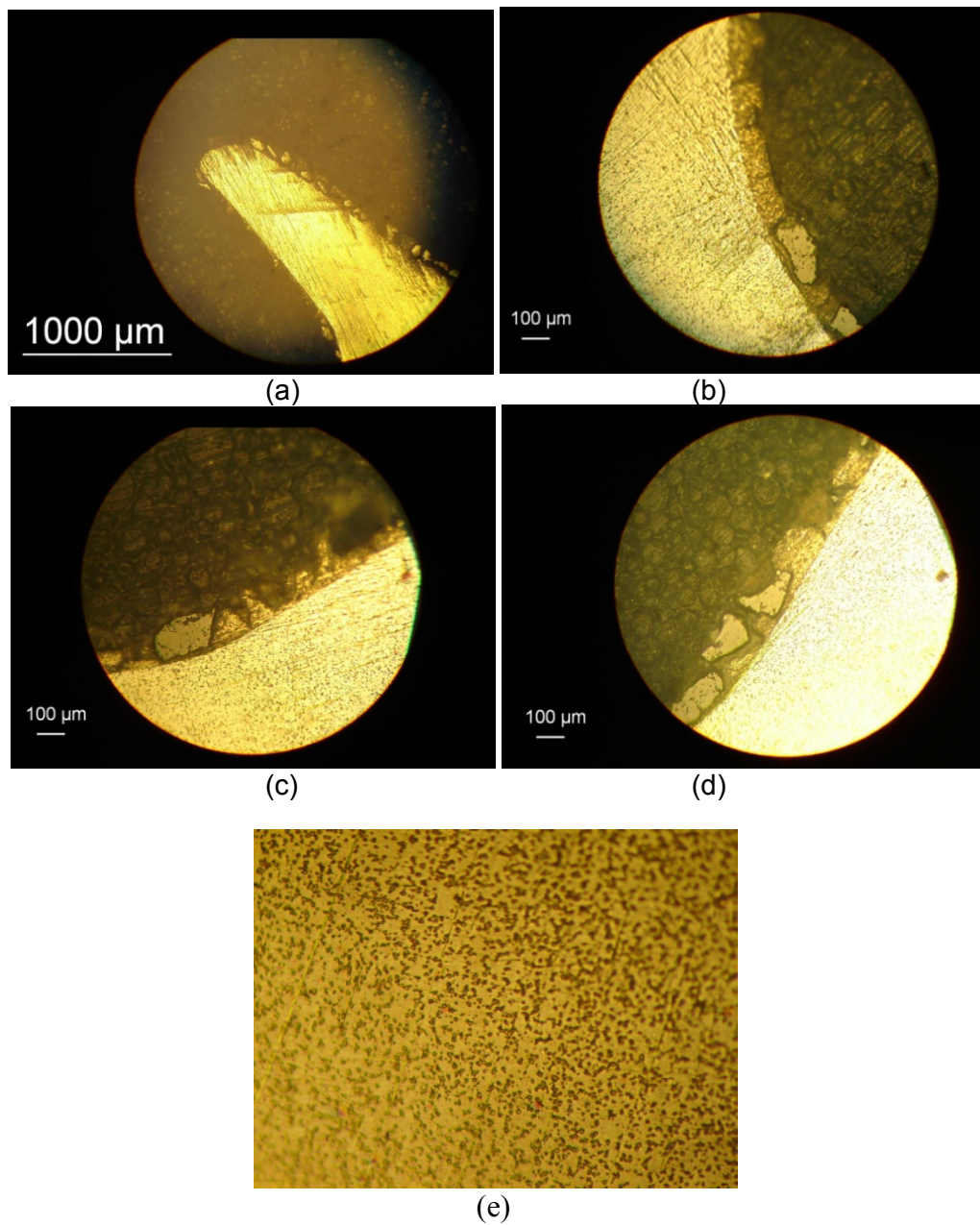


FIGURE 11. (a) Part of the thread with the worn coating. (b) Almost intact coating. (c)-(d) Coating showing grain removal and erosive wear. No cracks penetrating the substrate material were identified. (e) Microstructure of the substrate containing resolved precipitates (x250).

Here it has to be emphasized, that in real world the forward cooling plate, the rotor disk and the aft cooling plate although being fixed together, are allowed to expand due to temperature increase at bigger degree compared to the case simulated previously (total fixation); thus the thermal stress results presented in figure 12 represent a conservative solution. From the FEA results it is deduced that the critical sites for optical observation are located at the vicinity of holes of the flange where the fixations with the bolts exist, at the intersection of the flange and the thread and the thread as well. Notice, that the FEA results presented herein provide only a

global indication of some of the critical areas with respect to failure and are presented as supplementary information to the laboratory investigation results.

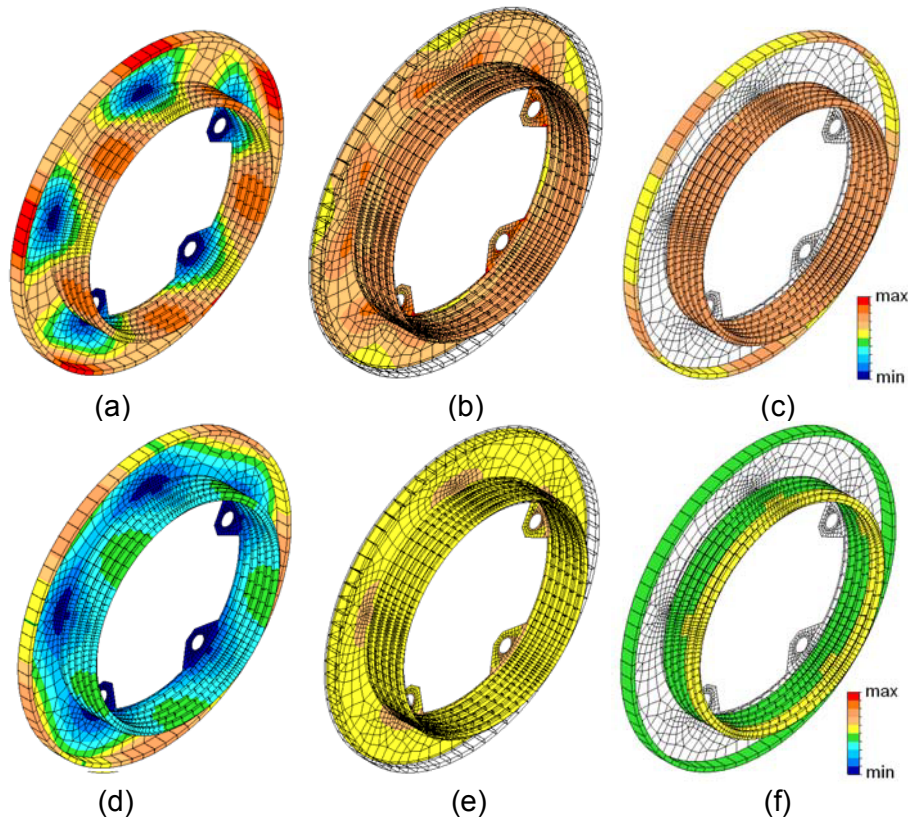


FIGURE 12. (a) LC1: Magnitude of displacements due to rotation. (b) LC1: Von Mises centrifugal stress on flat shells. (c) LC1: Worst centrifugal stress on beams. (d) LC2: Magnitude of displacements due to temperature increase. (e) LC2: Von Mises thermal stress on flat shells. (f) LC1: Worst thermal stress on beams.

DISCUSSION, CONCLUSION AND RECOMMENDED ACTIONS

From the findings of the current investigation the following are deduced:

- a. The plates are made from a coated high strength nickel superalloy [1, 2].
- b. The microstructure of the nickel matrix contained resolved precipitates.
- a. On the coating of the plates, nickel as long as aluminum, tungsten, silicon and iron were detected.
- b. Four out of eight plates exhibited worn coating at the thread (eroded or lost coating).
- c. One out of eight plates presented fractured coating at the thread (coating loss).
- d. One out of eight plates exhibited local plastic deformation and fracture of its structural elements.
- e. None of the eight cooling plates presented any cracking in macro scale that could be identified by naked eye or by using a typical laboratory stereo-microscope.
- f. Nondestructive testing did not reveal the existence of any crack in macro scale in any of the plates.

- g. Localized observation at all locations of the most strained plate using Scanning Electron Microscopy did not reveal any micro crack propagating through the substrate material of the plates.
- h. The most strained plate (stage 1 forward cooling plate) presented non-uniform wear of the coating on its flange. The latter is probably attributed to the contact with the joining machinery (see also figure 1). Erosive wear of its coating at the thread was identified. Extensive cracking of the eroded coating and coating loss was also observed.
- i. Microstructural analysis from a sample of the most strained plate (stage 1 forward cooling plate) confirmed the existence of severely worn, eroded, cracked and lost coating but did not identify any cracks penetrating through the substrate material. The thickness decrease of the coating at some areas was equal to 80%.

Nickel alloys are used for a wide variety of applications, the majority of which are designed to take advantage of the corrosion resistance and/or heat resistance properties of these alloys. Nickel superalloys are used in turbine compressor blades and discs, shafts, spacers, fasteners, miscellaneous jet engine hardware; space shuttle turbo pump seals, afterburner components, combustion chamber liners, nozzles, vanes, rings, turbine exhaust weldments, structural parts, etc [1, 2, 3]. Nickel is a versatile element and will alloy with most metals. Complete solid solubility exists between nickel and copper; wide solubility ranges between iron, chromium, and nickel make possible many alloy combinations. The face centered cubic structure of the nickel matrix (γ) can be strengthened by solid-solution hardening, carbide precipitation, or precipitation hardening. Cobalt, chromium, molybdenum, tungsten, titanium, and aluminum are all solid-solution hardeners in nickel. Aluminum, titanium and niobium are strong γ' -Ni₃(Al,Ti) and γ'' -Ni₃Nb precipitate formers, which when present in a high nickel matrix provide significant strengthening of the material. Tungsten, titanium, niobium, molybdenum and chromium act as carbide formers. Aluminum and chromium provide oxidation resistance [1-3]. Because high temperature failures normally initiate at the grain-boundary interfaces, it is a common practice to reduce the grain boundary interfaces or completely eliminate them [4].

The temperature at the entrance of the turbine can be considerably high. Therefore to keep the structural parts from degradation, both complex cooling schemes and coatings are often used. High temperature coatings are designed to increase the life of the underlying alloy during service. In general, nickel-based alloy coatings show good high-temperature wear and corrosion resistance. They have good wear resistance after adding tungsten and molybdenum elements to the alloy. Nickel based coatings are used in applications when wear resistance combined with oxidation or hot corrosion resistance is required [5-13]. Two generic coating types are used for similar applications: diffusion coatings and overlay coatings. Both types of coatings result in a surface layer enriched in oxide-forming elements to promote formation of a protective oxide layer. In general, the use of protective coatings can greatly increase the lives of nickel base superalloys for operating conditions in which the oxidation or hot corrosion resistance of the base material is unacceptable. However, the protective coatings themselves are subject to degradation under engine operating conditions and thus have limited lives. Degradation of the protective coating can affect the integrity of the substrate material leading to its failure [4-13].

From the results presented above it is finally deduced that the protective coating of the plates was degraded, eroded and lost in several areas, exposing the substrate material to the aggressive gas environment. It is thus concluded that, in spite of the fact that the plates seemed to be macroscopically in good condition, the identified wear may substantially contribute to onset of failure, as literature indicates [1,4-13].

The test protocol that was applied in current expert report has included Macroscopic investigation in combination with Non-destructive Inspection for identification of global distortion or defects, Microstructural analysis combined with Metallographic observation, Hardness testing and global Chemical Analysis for material characterization, Fractographic observation and local Chemical Analysis for identification of fractographic mechanisms realized in micro scale and finally Finite Element Analysis for better understanding of operational response. The results of the aforementioned tests and analyses that have been often employed in failure analyses can be used in order to assess the maintenance, repair and overhaul procedure of high reliability components.

ACKNOWLEDGMENTS

The authors would like to thank the military and civil personnel of the Telecommunication and Electronics Media Factory of the Hellenic Military Aviation for their help in conduction of the nondestructive testing and SEM/EDS analysis. Authors also acknowledge that current work was made possible by the assistance of the military personnel of the Hellenic Helicopter Naval Base.

REFERENCES

1. ASM handbook, Vol. 5, Surface Engineering; 1994.
2. ASM handbook, Vol. 2, Properties and Selection: Nonferrous Alloys and Special-Purpose Materials; 1990.
3. ASM handbook, Vol. 9, Metallography and Microstructures; 2004.
4. ASM handbook, Vol. 11, Failure Analysis and Prevention; 2002.
5. T.S. Sidhu, S. Prakash, R. D. Agrawal, Hot corrosion and performance of nickel-based coatings, *Current Science* 90 (2006) 41-47.
6. R. Sivakumar, B.L. Mordike, High temperature coatings for gas turbine blades: A review, *Surface and Coatings Technology* 37 (1989) 139-160.
7. AS. Osyka, AI. Rybnikov, S.A Leontiev, N.V. Nikitin, I.S. Malashenko, Experience with metal/ceramic coating in stationary gas turbines, *Surface and Coatings Technology* 76-77 (1995) 86-94.
8. G.W. Goward, Progress in coatings for gas turbine airfoils, *Surface and Coatings Technology* 108-109 (1998) 73-79.
9. N. Eliaz, G. Shemesh, R.M. Latanison, Hot corrosion in gas turbine components, *Engineering Failure Analysis* 9 (2002) 31-43.
10. M.J. Pomeroy, Coatings for gas turbine materials and long term stability issues, *Materials and Design* 26 (2005) 223-231.
11. I. Gurrappa, A. Sambasiva Rao, Thermal barrier coatings for enhanced efficiency of gas turbine engines, *Surface & Coatings Technology* 201 (2006) 3016-3029.
12. R. Rajendran, M.D. Ganeshachar, Jivankumar, T. Mohana Rao, Condition assessment of gas turbine blades and coatings, *Engineering Failure Analysis* 18 (2011) 2104-2110.
13. R. Rajendran, Gas turbine coatings – An overview, *Engineering Failure Analysis* 26 (2012) 355-369.